Chapter 5

Implications for Ultralow-velocity Zones

5.1 Physical Mixing Models

To explore the expected sound velocities and density of an ultralow-velocity zone containing iron-rich (Mg,Fe)O, we can construct simple models that combine the properties of iron-rich (Mg,Fe)O and mantle silicates. We show that a small amount of iron-rich (Mg,Fe)O can greatly reduce the average sound velocity of an aggregate assemblage. When combined with a geodynamic model of a solid ULVZ (*Bower et al.*, 2011), we can directly correlate inferred sound velocities to mineralogy and predicted ULVZ shapes. Our combined geodynamic and mineral physics model of a solid ULVZ can be used to explore the relationship between the observed sound velocities and mineralogy of ULVZs with added insight into ULVZ morphology.

5.1.1 Extrapolation of Magnesiowüstite properties to the CMB

Re-evaluation of sound velocities of $(Mg_{.16}Fe_{.84})O$ occurred after publication, which was presented unaltered in Chapter 2. Updates include a re-analysis of the sample, finding the composition to be $(Mg_{0.18}Fe_{0.78}Ti_{0.04})O$. In addition, we assume that equation of state of $(Mg_{.16}Fe_{.84})O$ can be approximated by that of $(Mg_{.06}Fe_{.94})O$, rather than that of $(Mg_{.12}Fe_{.78})O$. This equation of state choice should be more self-consistent, as both samples were made in the exact same way. Updated Debye velocities of $(Mg_{.16}Fe_{.84})O$ are shown in Figure 5.1, underlying those of $(Mg_{.06}Fe_{.94})O$ and

FeO presented in Chapter 3.

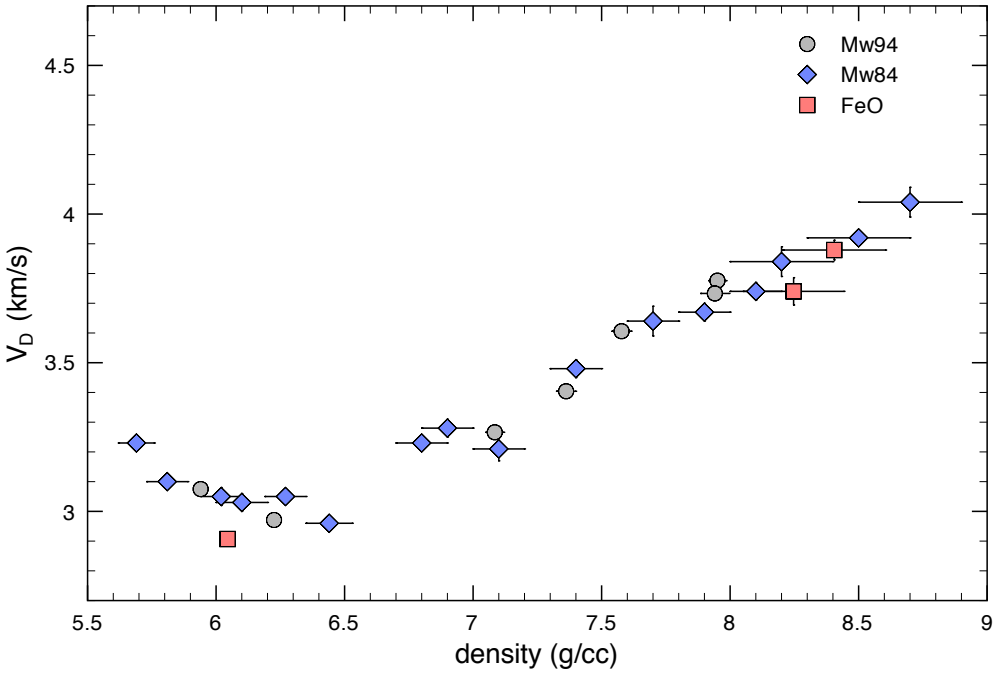

Figure 5.1: Debye velocity as a function of density of $(Mg_{.16}Fe_{.84})O$, $(Mg_{.06}Fe_{.94})O$, and FeO. $(Mg_{0.06}Fe_{0.94})O$ volumes were measured in-situ at Sector 3-ID-B of the Advanced Photon Source (APS). The volumes of FeO were measured at Sector 12.2.2 of the Advanced Light Source (low density) and at Sector 13-ID-D of the APS (high density). The volumes of $(Mg_{0.16}Fe_{0.84})O$ above ambient pressure were not measured, but estimated using ruby pressure, initial volume measured at the ALS, and the equation of state parameters $(Mg_{.06}Fe_{.94})O$: of $K_{0T} = 189(4)$ GPa and $K'_{0T} = 2.9(1)$. Figure updated from Figure 3.12 to include recalculated $(Mg_{.16}Fe_{.84})O$.

The Debye velocities in Figure 5.1 exhibit a linear increase as a function of density above 6.5 g/cc, independent of composition. As the highest density of $(Mg_{.16}Fe_{.84})O$ at 8.7 g/cc corresponds to a pressure of 121 GPa, we extrapolate that this linear trend is valid up to the core-mantle boundary pressure of 135 GPa.

In the latest formulation of the mixing model, presented below, the Debye sound velocities of $(Mg_{.06}Fe_{.94})O$ are linearly extrapolated to 135 GPa. This choice is made for self-consistency reasons, as it is the only dataset with in-situ volumes mapped directly onto its own equation of state. Here we assert that the Debye sound velocity as a function of density of $(Mg_{.16}Fe_{.84})O$ is the same as that of $(Mg_{.06}Fe_{.94})O$, since we cannot discern a difference. This assumption, however, introduces a slight inconsistency in the parameterization of Debye velocity with other compositions, which will

have to be worked out before this model can be published. Namely, this simple extrapolation to the CMB gives a $(Mg_{.16}Fe_{.84})O$ density of 8.63 g/cc, which is lower than the highest density plotted in Figure 5.1.

We estimate the sound velocities of $(Mg_{.16}Fe_{.84})O$ at high temperature by using the temperature derivatives $\partial V_P/\partial T = -4.64\times10^{-4}$ (km s^{-1}K^{-1}) and $\partial V_S/\partial T = -3.85\times10^{-4}$ (km s^{-1}K^{-1}), measured for MgO up to 20 GPa and 1650 K (*Kono et al.*, 2010). Density is adjusted for high temperature using the equation of state we measured on buffered $(Mg_{.06}Fe_{.94})O$ (Chapter 4, Table 4.3).

5.1.2 Mixture of Magnesiowüstite and Ambient Mantle

One such model represents a mixture of iron-rich (Mg,Fe)O and ambient mantle, and is hereafter referred to as "Mw+PREM". Prior versions of this model were published in *Wicks et al.* (2010) (Chapter 2) and updated in *Bower et al.* (2011), and mixes iron-rich oxide with surrounding lower mantle represented by the Preliminary Reference Earth Model (PREM) (*Dziewonski and Anderson*, 1981). This binary mixture can be thought of as a disequilibrium assemblage of lower mantle material mixed with iron-rich oxide.

Considering a physical mixing scenario in which an iron-rich oxide is combined with ambient mantle has two advantages. First, it is generally accepted that a large fraction of the lower mantle is made up of silicate perovskite, due to the fact that the expected sound velocities and density of perovskite largely agree with PREM. Using the seismic velocities and densities of PREM, therefore, should be a good approximation to using sound velocities and densities of perovskite, although it likely represents a mixture of phases. Second, without knowing the mechanism by which a ULVZ is formed, it is conceivable that a ULVZ can simply be a mixture of lower mantle and core material. There is increasing evidence for complexity on the core side of the core-mantle boundary which could be an expression of exsolved "sediments" on the top of the core (*Buffett et al.*, 2000). Therefore, a ULVZ could simply be ambient mantle mixed with FeO, which is what this mixing model represents.

We then calculate the Voigt and Reuss bounds for V_P, V_S, and density (*Watt et al.*, 1976) for a

Table 5.1: Model parameters for mixing model "Mw+PREM"

	V_P (km/s)	V_S (km/s)	density (g/cc)
PREM	13.714	7.2648	5.5613
Mw84 (2700 K)	7.3014	2.705	8.3001
Mw84 (4700 K)	6.3734	1.935	8.2288

given vol% of $(Mg_{.16}Fe_{.84})O$ and PREM at 135 GPa, choosing a low (2700 K) and high (4700 K) temperature estimates of the core-mantle boundary (Figure 5.2). Model parameters are listed in Table **??**. Voigt (uniform stress) and Reuss (uniform strain) bounds bracket the upper and lower bounds of mixing of the bulk modulus K, shear modulus G and density ρ, from which we calculate V_P and V_S using Equation 2.2 and $G = \rho V_S^2$.

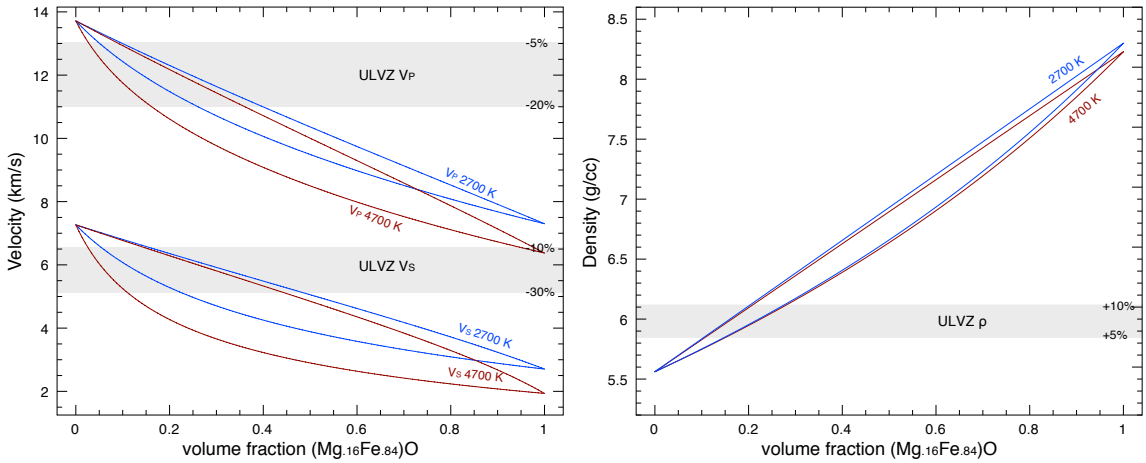

Figure 5.2: Voigt (upper)-Reuss (lower) bounds of V_P, V_S (left), and density (right) of $(Mg_{.16}Fe_{.84})O$ with PREM at 135 GPa. Gray shading shows typical ULVZ velocities (-5-20% V_P, -10-30 %V_S, with respect to surrounding mantle) reported by seismology. Density is not very well constrained by seismology, but have been quoted at +8-10% (*Rost et al.*, 2006; *Idehara et al.*, 2007, e.g.). Dynamic models such as those by *McNamara et al.* (2010) predict ULVZs with densities of at least +5% with respect to surrounding mantle, yet models by *Bower et al.* (2011) create reasonable ULVZs corresponding to less than 5% density increase.

To first order, mixing of just 20 vol% of $(Mg_{.16}Fe_{.84})O$ with 80 vol% silicates (represented here by PREM) matches signature seismic observations for the ULVZ (Figure 5.2).

5.1.3 Mixture of Magnesiowüstite and Silicate Perovskite

A second mixing model, a prior version of which is published in *Bower et al.* (2011), again starts with the assumption that iron-rich oxide is present in a ULVZ and explores a possible equilibrium

assemblage of iron-rich (Mg,Fe)O and perovskite. Hereafter we refer to it as "Mw+Pv".

The partitioning behavior of Fe vs. Mg between the two phases has been probed at lower mantle pressures by numerous studies without much agreement, but recent studies show a preferential partitioning of Fe into the oxide phase, which we adopt: $K_D^{Pv/Mw} \approx 0.07$ (*Auzende et al.*, 2008; *Sakai et al.*, 2009; *Sinmyo et al.*, 2008), assuming an aluminum-free system. In addition to representing the simple phase assemblage that we model in this mixture, a low $K_D^{Pv/Mw}$ is required by this exercise in order to achieve reasonable densities for appropriate velocity decrements. In other words, too much iron in perovskite would create ULVZs denser than those consistent with observed heights, with velocities that are not low enough.

Other studies find the partitioning behavior to be less extreme, determining $K_D^{Pv/Mw} \approx 0.42$ for an assumed "pyrolite" mantle composition, or $K_D^{Pv/Mw} \approx 1.11$ in the presence of post-perovskite (*Sinmyo et al.*, 2011). Partitioning behavior is known to be a function of composition, pressure, and the presence of post-perovskite, but with opposite conclusions between even the most recent studies, $K_D^{Pv/Mw}$ is still an uncertainty (*Sinmyo et al.*, 2011; *Catalli et al.*, 2009).

If we assert that $(Mg_{.16}Fe_{.84})O$ exists at the core-mantle boundary, a coexisting perovskite in equilibrium would have the composition $(Mg_{.72}Fe_{.28})SiO_3$, using $K_D^{Pv/Mw} \approx 0.07$ (*Sakai et al.*, 2009; *Auzende et al.*, 2008). This resulting assemblage is very Fe-rich, and would require a formation mechanism capable of making such an exotic composition. We model the densities and sound velocities of perovskite using a finite-strain model given by *Li and Zhang* (2005), making a compositional correction to the density. Bulk and shear moduli have also been predicted to be compositionally-dependent (*Kiefer et al.*, 2002), but we found the resulting differences to be negligible (*Bower et al.*, 2011).

We calculate the Voigt and Reuss bounds for V_P, V_S and density for a given vol% of $(Mg_{.16}Fe_{.84})O$ and $(Mg_{.72}Fe_{.28})SiO_3$ perovskite at 135 GPa and 2700 and 4700 K (Figure 5.3).

The resulting mixing model is presented in Figure 5.3. Here, at $X_{(Mg,Fe)O} = 0$, we see the temperature dependence of the modeled perovskite in both velocities and densities of the silicate fraction. The range of expected perovskite velocity at the two extreme temperature estimates is

Table 5.2: Model parameters for mixing model "Mw+Pv"

	V_P (km/s)	V_S (km/s)	density (g/cc)
Pv (2700 K)	14.013	7.4287	5.7157
Pv (4700 K)	13.57	6.9129	5.4935
Mw84 (2700 K)	7.3014	2.705	8.3001
Mw84 (4700 K)	6.3734	1.935	8.2288

much larger than the difference between perovskite and PREM, which falls between the two. We conclude that the choice of silicate model (PREM vs (Mg,Fe)SiO_3) then is not distinguishable given the uncertainty in temperature of the CMB region.

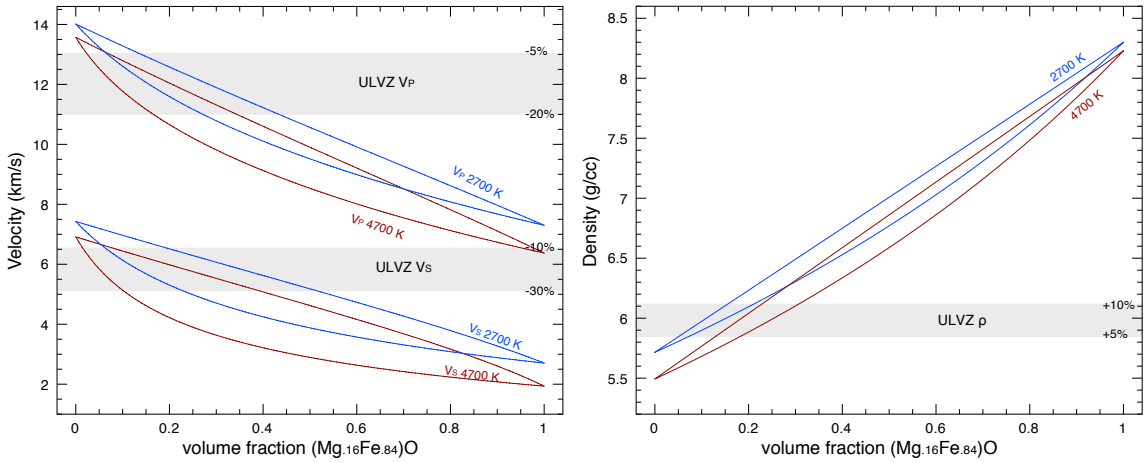

Figure 5.3: Voigt (upper)-Reuss (lower) bounds of V_P, V_S (left), and density (right) of $(Mg_{.16}Fe_{.84})O$ with (Mg,Fe)-perovskite. Gray shading same as in Figure 5.2

In both this model and in Mw+PREM, we find that only about 20% iron-rich magnesiowüstite is needed to drop the sound velocities of an assemblage. The density of perovskite is higher than PREM at 2700, but lower at 4700, so the density of Mw+Pv is greatly affected by temperature choice. As a result, the amount of Mw85 needed to match reported densities according to seismic studies jumps from 15% at 2700 K to 25% at 4700 K.

5.1.4 Dynamics of a Solid-state ULVZ

The mixing models described above show that ULVZ velocities and densities can be adequately represented by a mixture of iron-rich (Mg,Fe)O and perovskite or silicate-rich surrounding mantle. We can take this model one step further by interpreting these models in the context of dynamic

models (*Bower et al.*, 2011, specifically).

We explored the morphologies of solid-state ULVZs in a two-dimensional dynamic model, solving the steady-state thickness and shape of ULVZs as a function of prescribed initial thickness and chemical vs. thermal buoyancy (*Bower et al.*, 2011). By exploring a range of thicknesses and buoyancy numbers B, this study creates a range of candidate ULVZ sizes and shapes that can be mapped to mineral physics models via density and assumed temperature drop across the core-mantle thermal boundary layer, according to the definition of buoyancy number: $B = \frac{Rb}{Ra} = \frac{\Delta\rho_{ch}}{\rho\alpha\Delta T}$, where $\frac{Rb}{Ra}$ is the ratio of chemical to thermal Rayleigh numbers, $\Delta\rho_{ch}$ is the chemical density anomaly of the ULVZ layer, ρ and α are density and thermal expansion of the mantle, and ΔT is the temperature drop across the CMB. More detailed descriptions of the dynamic models are found in *Bower et al.* (2011).

Taking the density calculations of the two mixing models, and assuming a lower bound of ΔT_{CMB} of 500 K and an upper bound of ΔT_{CMB} =1500 K across the thermal boundary layer just above the core-mantle boundary, the range of dynamic models of *Bower et al.* (2011) map to volume fractions of $\sim 0.01 - 0.26$ of $(Mg_{.16}Fe_{.84})O$ for the Mw+PREM model, and $\sim 0.03 - 0.29$ for the Mw+Pv model. These models introduce a new kind of constraint: a much smaller density contrast, and therefore smaller amount of iron-rich (Mg,Fe)O, creates shapes with larger aspect ratios (height/width), whereas a larger density contrast and more iron-rich (Mg,Fe)O generally creates ULVZs that are flat yet wide. A seismic study that constrains the width and size of ULVZs now has a way to constrain density, assuming a solid mixed component.

A recent review of the core mantle boundary suggests that a CMB temperature of $\sim$ 4000 K and a temperature drop across the CMB thermal boundary layer of $\sim$1200-1800K (*Tackley*, 2012) best satisfies combined seismological and mineral physics constraints.Our mixing models, then, can be recalculated at a CMB temperature of 4000 K and ΔT_{CMB} of 1500 K to predict ULVZ morphologies. We plot the Voigt-Reuss-Hill curves in Figure 5.4.

It's important to note that the assumptions we made in these models can be revised as more is learned about the temperature and mineralogy of Earth's core-mantle boundary. The high-iron

Table 5.3: Model parameters for mixing model "Mw+PREM" and "Mw+Pv" at 4000 K

	V_P (km/s)	V_S (km/s)	density (g/cc)
PREM	13.714	7.2648	5.5613
Pv (4000 K)	13.712	7.0886	5.5795
Mw84 (4000 K)	6.6982	2.2045	8.23

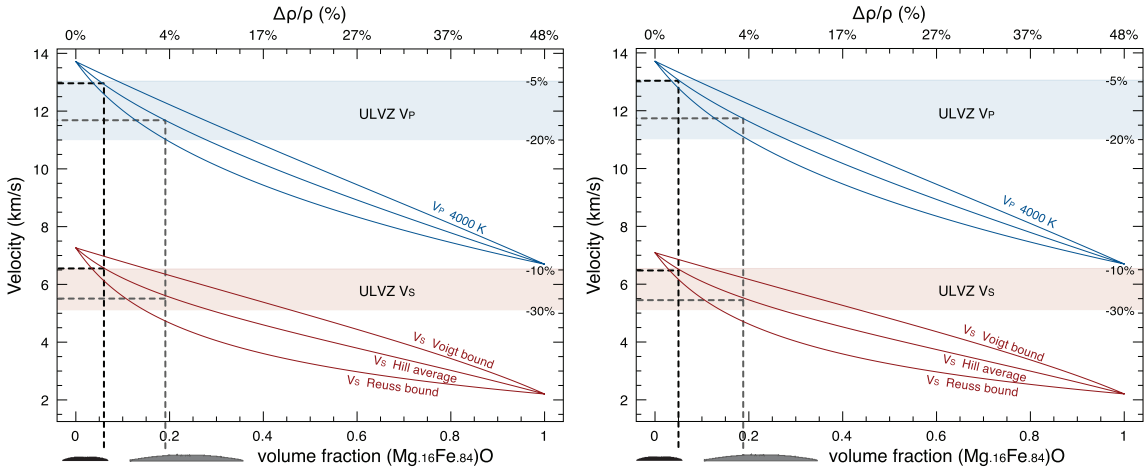

Figure 5.4: Voigt-Reuss-Hill curves of V_P and V_S of the mixing of $(Mg_{.16}Fe_{.84})O$ with PREM (left) and (Mg,Fe)SiO_3-perovskite (right), at T_{CMB} = 4000 K. Assuming an average temperature drop across the CMB thermal boundary layer of ΔT_{CMB} = 1500K (*Tackley*, 2012), ULVZs with moderate velocity drops are consistent with 5% (Mg,Fe)O, and are consistent with smaller structures with high aspect ratio from *Bower et al.* (2011). ULVZs with larger velocity drops are consistent with $\sim$ 20% (Mg,Fe)O, and are consistent with wider, flatter structures. At a CMB temperature of 4000 K, the ULVZ shapes predicted by PREM vs perovskite are indistinguishable (left and right panels, respectively).

content of a (Mg,Fe)O+Pv assemblage is too dense to explain ULVZs at cool temperatures, but adequately explains ULVZs at high temperatures (*Bower et al.*, 2011). Knowing both the absolute temperature and the temperature drop across the thermal boundary layer would allow us to compare different scenarios as a function of density.

Further studies on the mineral properties of mantle phases at high temperature are also required. One example is the extrapolation of sound velocities with temperature. Very few studies exist that measure the velocity derivatives of MgO at high temperature, and none exist in the iron-bearing system. The velocity derivatives we used, measured up to 20 GPa and 1650 K, $\partial V_P/\partial T = -4.64\times10^{-4}$ (km $s^{-1}K^{-1}$) and $\partial V_S/\partial T = -3.85\times10^{-4}$ (km $s^{-1}K^{-1}$) (*Kono et al.*, 2010), are slightly lower than those measured on MgO at room pressure, $\partial V_P/\partial T = -6\times10^{-4}$ (km $s^{-1}K^{-1}$) and $\partial V_S/\partial T = -5\times10^{-4}$ (km $s^{-1}K^{-1}$) (*Sinogeikin et al.*, 2000). Applying these velocity derivatives at

121 GPa is likely overestimating the velocity drop with temperature. The effect of applying these velocity derivatives to iron-rich (Mg,Fe)O rather than MgO is unknown.

5.2 Conclusions

In this work, we have experimentally determined the room temperature sound velocities of $(Mg_{0.16}Fe_{0.84})O$ and $(Mg_{0.06}Fe_{0.94})O$ as a function of pressure up to 121 GPa. We found that the trend in sound velocities was very strongly affected by magnetic transitions: by monitoring the magnetic state using synchrotron Mössbauer spectroscopy, we identified softening in the shear elastic properties of iron-rich (Mg,Fe)O preceding a magnetic transition.

We have also presented the pressure-volume-temperature equation of state of $(Mg_{0.06}Fe_{0.94})O$ up to 115 GPa and 1900 K, measured both with and without an in-situ Fe buffer, and showed that we could not conclusively distinguish the two equations of state. This result is consistent with other studies of the (Mg,Fe)O solid solution that propose pressure-induced exsolution of Fe^{3+}, essentially "self-buffering" (*Zhang and Zhao*, 2005; *McCammon et al.*, 1998). This result is important for practical reasons, as future high-temperature NRIXS studies will not need to have an in-situ buffer.

The work we have completed forms the foundation for future experiments at high temperature. The room temperature sound velocities as a function of pressure form the reference curve for high temperature comparison, and the equation of state as a function of pressure and temperature is required to determined in-situ pressure of a high temperature velocity measurement.

We combined the sound velocities and P-V-T equation of state to predict the properties of iron-rich (Mg,Fe)O at high temperature, and made mixing models to predict the properties of example phase assemblages. Our overall conclusion, with different choices of mixing model, stayed the same: mixing small amounts of iron-rich (Mg,Fe)O with mantle silicate reproduces the characteristic sound velocities and shapes of ultralow-velocity zones.